PHYSICAL REVIEW B VOLUME 41, NUMBER 12 15 APRIL 1990-II

Influence of surface corrugations on hydrogenic image-potential states

Clinton DeW. Van Siclen
Idaho National Engineering Laboratory, P.O. Box 1625, Idaho Falls, Idaho 83415
(Received 21 November 1989)

An electron can be bound to a surface by the Coulomb attraction to its positive image charge. The resulting Rydberg-type series of image-potential surface states has been observed in the band gaps of free-electron-like *s,p* bands for several metal surfaces. The binding energy for the first member of the series ($n=1$) is very nearly hydrogenic for the dense (111) crystallographic surfaces, but appears to depart significantly from the hydrogenic value for the more strongly corrugated (100) surfaces. Variational calculations are performed to determine the energy-level shifts due to surface corrugations, assuming a simple model potential and coincident image plane, hard-wall boundary, and corrugated surface. The binding energy is found to be decreased only slightly by the surface structure, contrary to recent theoretical results obtained by perturbation theory, but consistent with the standard phase-shift analysis of the experimental data.

I. INTRODUCTION

Image-potential states appear to be a universal feature at metal surfaces. An electron may be bound to the surface by the Coulomb attraction to its induced image charge, but prevented from escaping into the crystal by the existence of a band gap of bulk states around the vacuum level (Fig. 1). The long-range Coulombic potential gives rise to a series of Rydberg-like energy levels converging towards E_{vac} for zero parallel (to the surface) momentum $k_{\parallel}$ of the electron. These energies will differ from their hydrogenic values,

$$E_n = -(1\ \text{Ry})/(16n^2),\quad n=1,2,3,\dots, \tag{1}$$

to a greater or lesser degree depending upon the strength of the coupling of the image-potential states to the crystal.

Intuitively, one would expect the coupling to be rather weak, since the wave functions protrude far out into the vacuum region. For example, the ground-state hydrogenic wave function $\psi_{n=1}(z)=8z\exp(-z/4)$ (z is in units of Bohr radii), which attains its maximum amplitude a distance 2.1 Å from the perfectly conducting surface at $z=0$. Excited-state wave functions, having greater spatial extent, should be even less influenced by crystal properties.

Precise measurements of the image-potential ground-state binding energies for the (111) and (100) crystallographic surfaces of Cu, Ag, and Ni have recently been made by Giesen *et al.*[1-4] using two-photon photoemission spectroscopy. A comparison of their results collected in Table I shows that for a given crystallographic structure, the binding energy is essentially independent of the material. The different crystalline surfaces, however, give markedly different binding energies, decreasing from the nearly hydrogenic value (0.85 eV) of 0.8 eV for the smooth (111) surfaces to approximately 0.55 eV for the corrugated (100) surfaces. These trends are generally followed in the experimental data for various other metals and surfaces measured by other groups and recorded by Straub and Himpsel[5] in their Table I.

The observed binding energies clearly require that corrections be made to the simple hydrogenic model. These may be of two types: (i) modification of the image potential in the z direction, and (ii) consideration of surface corrugation.

A realistic image potential must "saturate" at the crystal surface—that is, it must make a smooth transition to the bulk potential as the many-body screening processes

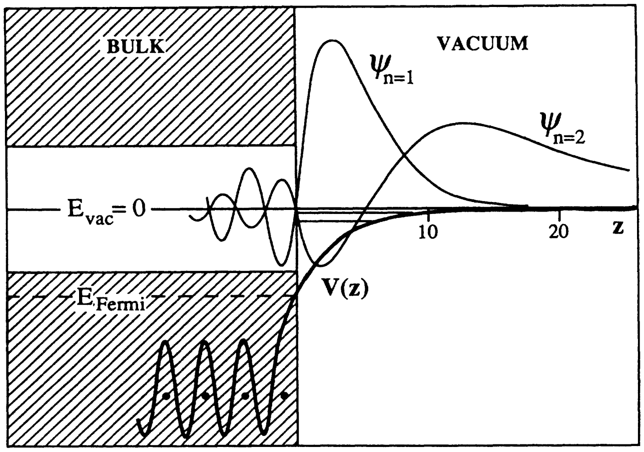

FIG. 1. Illustration of the ground and first excited image-potential electronic states at a metal surface. These exist due to the long-range Coulombic attraction between the electron in the vacuum and the induced surface charge, and the presence of a bulk band gap around the vacuum level E_{vac} that prevents the electron from combining with the metal. The crystal and image potentials $V(z)$ join smoothly at the surface; in the calculations reported here, the metal is regarded as perfectly conducting so that the image potential goes to negative infinity at the surface.

TABLE I. Experimentally determined binding energies (in eV) for image-potential states at Cu(111), Ag(111), and Ni(111) and (100) crystallographic surfaces.

	Crystallographic surface	
Metal	(111)	(100)
Cu	0.83 ± 0.03^{b}	0.57 ± 0.02^{c} 0.18 ± 0.02^{c} $(n=2)$
Ag	$0.77\pm0.03^{a,b}$ 0.23 ± 0.03^{a} $(n=2)$	0.53 ± 0.02^{c} 0.16 ± 0.02^{c} $(n=2)$
Ni	0.80 ± 0.03^{b}	

[a] Reference 1.
[b] Reference 2.
[c] Reference 3.

come into play near the surface. This effect is included in a model most simply by requiring the potential inside the crystal to abruptly terminate at half an interlayer outside the last layer of surface atoms, remain constant at that value for a distance of roughly 0.2 Å, and then merge with the Coulomb image potential, which of course has the correct asymptotic behavior (see, for example, Ortuño and Echenique[6]). The arbitrary parameter is the width of the constant-potential region, or equivalently, the distance z_{im} of the image plane (at which the hydrogenic potential becomes infinite) from the surface. Very good qualitative results for the image-state binding energies have been achieved by Smith[7,8] using such a model potential in a phase-shift analysis based on earlier work by Echenique and Pendry.[9] In this theory, the image-potential states obey the Bohr-like quantization condition

$$\phi_C+\phi_B=2\pi n, \quad n=1,2,3,\ldots, \tag{2}$$

on the round-trip phase accumulated by the electron wave function as it travels between the crystal and the Coulomb barrier. ϕ_C and ϕ_B are the phase changes due to reflection at the crystal-band-gap barrier and at the image-potential barrier, respectively. The phase shift ϕ_C depends upon the position of the energy level in the band gap, varying (for $n=1$) from 0 at the bottom of the gap to π at the top of the gap. The phase shift at the band-gap-barrier and saturation of the image potential can be included in a simple one-dimensional model by introducing a quantum defect a_n in the expression for the image-state energies E_n:

$$E_n=-(1\ \mathrm{Ry})/[16(n+a_n)^2], \quad n=1,2,3,\ldots, \tag{3}$$

where $a_n=(1-\phi_C/\pi)/2$ (Ref. 10). For the Cu(111), Ag(111), and Ni(111) surfaces, the vacuum level lies near the top of the bulk band gap, giving $\phi_C\cong\pi$ and binding energies $E_{n=1}\cong0.85$ eV and $E_{n=2}\simeq0.21$ eV from the expression above; for the (100) surfaces, the vacuum level is at midgap, giving $\phi_C\cong\pi/2$ and $E_{n=1}\cong0.54$ eV and $E_{n=2}\cong0.17$ eV. The close agreement between these results and the measurements in Table I provides strong support for the phase-shift analysis. Further experimental evidence for very weak coupling to the crystal electronic states includes the narrow widths of the image-potential states (less than 0.1 eV), and their persistance as surface resonances in the presence of bulk states [as in the case of Au(111) (Ref. 5)].

It is not inconceivable, however, that surface corrugations (periodic variations in charge density at the crystal surface reflecting the underlying ionic structure) could contribute significantly to the shift of the image-state energy levels from their hydrogenic values, particularly since typical corrugation heights are roughly the size of the distance z_{im} derived from experiment using the phase-shift analysis. Garcia *et al.*[11] observed an image-potential state 0.6 eV below the vacuum level for the Ag(100) surface by inverse photoemission spectroscopy, which they interpreted as the $n=2$ state "pulled down" by the influence of the corrugation potential. According to their second-order perturbation theory calculation, the binding energy is expected to increase with increasing corrugation. Binnig *et al.*[12] studied image-potential surface states of Ni(100) by tunneling spectroscopy, and concluded that non-free-electron motion along the surface plays an essential role in the binding of the image states. Clinton *et al.*[13] considered both the image potential and boundary condition to be perturbed from their hydrogenic, flat-plane expressions, and applied second-order perturbation (in the corrugation height) theory to determine modified image-state wave functions. Using corrugation heights in the range 0.15–0.3 Å, they calculated upward ground-state energy shifts of approximately 0.11–0.16 eV for the (100) surfaces of Cu, Ag, and Au. (The use of wave functions and an image potential constructed under the requirement that the corrugation height be small in comparison to, for example, the spatial extent of the ground-state wave function, but showing such significant sensitivity to the surface structure, makes these results difficult to assess.) These conclusions are contradicted, however, by Hulbert *et al.*,[14] who derived the image states for the Cu(100) surface by matching a long-range image potential onto a self-consistent crystal potential determined by a first-principles full-potential linearized augmented-plane-wave calculation, and found no appreciable effect on the binding energy when surface corrugations were "turned off."

While the success of the phase-shift analysis in producing image surface-state energies in good agreement with experiment is impressive, it nonetheless seems worthwhile to consider further the effects of surface corrugation on the energy levels. This paper reports on variational calculations to determine the energies of image-state wave functions coupled to a corrugated, perfectly conducting surface by a simple, hydrogenic-like potential. The variational method permits calculation of a selected energy level to arbitrary accuracy by effectively arranging the image-state charge density over the hills and valleys of the surface to produce the minimum energy. Because the wave functions are forced to respond to the periodicity of the surface (which coincides with the image plane) both by the image potential and by the requirement that they vanish there, the calculated energies should exaggerate the degree to which surface corrugation may affect image-potential energy levels of real crystal surfaces.

II. VARIATIONAL METHOD

The variational method is well suited to this problem of determining the spectrum of image surface-state energies, primarily because it permits the boundary conditions to be incorporated in a very simple way. The brief description of the method that follows is taken largely from MacMillen and Landman,[15] who applied it to a model of physisorption at a planar surface, and from Epstein.[16]

The variational principle for eigenvalues is

$$\delta[E]=\delta\left[\left[\int \psi^{*}\mathbf{H}\psi\, dV\right]\Big/\left[\int \psi^{*}\psi\, dV\right]\right]=0\ , \qquad (4)$$

where **H** is the Hermitian operator of the eigenvalue equation

$$\mathbf{H}\psi=E\psi\ , \qquad (5)$$

and the function ψ obeys the boundary conditions. For the present problem, ψ must vanish at the corrugated boundary, so that is convenient to write the trial function as the combination

$$\psi(\mathbf{r})=G(\mathbf{r})\sum_{n} A_n\phi_n(\mathbf{r})\ , \qquad (6)$$

where $G(\mathbf{r})$ is a "cutoff" function that vanishes at the boundary, the A_n are the linear variation parameters, and the set $\phi_n(\mathbf{r})$ satisfies the boundary conditions of the simpler planar problem (all ϕ_n vanish at a planar surface). The subscript n represents all the quantum numbers that characterize the basis set of the system.

The trial function is expanded in a basis set that will not in general be orthogonal because of the presence of the factor $G(\mathbf{r})$ and the integration over a truncated space. The variation of the linear parameters A_n will then lead to the generalized matrix eigenvalue problem

$$\mathbf{H}\,\mathbf{A}=E\mathbf{N}\,\mathbf{A}\ , \qquad (7)$$

involving an overlap matrix **N**. The Hermitian matrices **H** and **N** have matrix elements

$$(\mathbf{H})_{n'n}=\int_T [G(\mathbf{r})\phi_{n'}]^{*}\mathbf{H}[G(\mathbf{r})\phi_n]dV \qquad (8)$$

and

$$(\mathbf{N})_{n'n}=\int_T [G(\mathbf{r})\phi_{n'}]^{*}[G(\mathbf{r})\phi_n]dV\ , \qquad (9)$$

the subscript T on the integrals indicating integration over the truncated space. The orthonormality condition satisfied by the vectors $\mathbf{A}_n$ is

$$(\mathbf{A}^{\dagger}\mathbf{N}\,\mathbf{A})_{n'n}=\delta_{n'n}\ . \qquad (10)$$

Because the set of basis functions forms a linear space, the set of successive energies E obtained by solving the matrix equation are upper bounds to the corresponding successive eigenvalues of **H**. This procedure may be improved by incorporating an additional variational parameter β in the set of functions $\phi_n(\mathbf{r})$, and applying the variational condition $\partial[E]/\partial\beta=0$. In practice, a value for β is chosen, and the generalized matrix equation is solved yielding the eigenvalues and eigenvectors. This step is repeated in a systematic way for different values of β until the eigenvalue of interest cannot be lowered further within the desired accuracy.

III. CALCULATION OF ENERGY LEVELS

The Hamiltonian for the image-potential surface states is

$$\mathbf{H}=-\nabla^2+V(\mathbf{r})\ , \qquad (11)$$

with distances and energies in units of Bohr radii ($a_0=\hbar^2/me^2$) and Rydbergs ($e^2/2a_0$), respectively. For an electron above an idealized, planar conducting surface at $z=0$, the image potential $V(z)=-1/2z$. Periodic surface corrugations produce an identical periodicity in the potential and in the wave functions, so that the Schrödinger's equation to be solved is

$$\left[-\frac{\partial^2}{\partial x^2}-\frac{\partial^2}{\partial z^2}+V(x,z)\right]\psi(x,z)=E\psi(x,z) \qquad (12)$$

for corrugations running parallel to the y axis. In these calculations, the wave function ψ vanishes at the sinusoidal surface $z=A[1-\cos(\omega x)]$ and interacts with that surface through the potential

$$V(x,z)=-(2\{z-A[1-\cos(\omega x)]\})^{-1}\ . \qquad (13)$$

This model potential, which is similar to that used by Shikin[17] to study thermal surface excitations in liquid helium by considering their interaction with surface electronic states, and by Nieminen and Puska[18] in their study of positron surface states, has the correct behavior at the perfectly conducting surface and at infinity, and is felt to be adequate for these calculations.

The trial wave function $\psi(x,z)$ is constructed from the set of basis functions having the form

$$\psi_{m,n}(x,z;\beta)=G(x,z)\cos(m\omega x)\phi_n(\beta z)\ , \qquad (14)$$

with $m=0,1,2,\ldots$ and $n=1,2,3,\ldots$, where the boundary condition is imposed by the cutoff function

$$G(x,z)=z-A[1-\cos(\omega x)]\ , \qquad (15)$$

and the one-dimensional hydrogenlike functions

$$\phi_n(\beta z)=e^{-\beta z/2}zL^{1}_{n-1}(\beta z)\ . \qquad (16)$$

The (unnormalized) ϕ_n differ from the exact wave functions for the smooth conducting surface problem[19,20] by the replacement $z\rightarrow\beta z$; the subscript n is the quantum number that distinguishes eigenstates of the smooth surface problem when the scale factor $\beta=1/2n$. The L functions are associated Laguerre polynomials.

The factor $\cos(m\omega x)$ imposes the periodicity of the surface on the basis functions. Due to the independence of the m and n indices, the energy minimization procedure described in Sec. II and below automatically produces a wave function $\psi(x,z)$ whose charge density is optimally distributed over the hills and valleys of the surface.

Calculation of an energy level now proceeds as follows.

(i) A set of $(M+1)N$ basis functions $\psi_{m,n}$ ($m=0,1,\ldots,M$ and $n=1,2,\ldots,N$) and an initial value for the variational parameter β are chosen.

(ii) Elements of the $(M+1)N\times(M+1)N$ Hamiltonian matrix $\mathbf{H}$ and overlap matrix $\mathbf{N}$ are calculated, the z integrations taken over the range $\{A[1-\cos(\omega x)],R\}$ and the x integrations taken over the period $[0,2\pi/\omega]$. The distance R is chosen to be somewhat greater than that required to reproduce the correct eigenvalue E_N for the planar conductor problem (with $A=0$), so that integration over the entire trial wave function is assured. Only $(M+1)N[(M+1)N+1]/2$ matrix elements of $\mathbf{H}$ and of $\mathbf{N}$ must be calculated due to the hermicity of the matrices.

(iii) The generalized matrix eigenvalue equation is solved numerically for the $(M+1)N$ eigenvalues. These are arranged in N sets (or "bands") of $M+1$ values, the lowest eigenvalue of the nth set corresponding to the best upper energy bound to E_n.

(iv) A new value for β is chosen, and steps (ii) and (iii) are repeated. This procedure continues until the selected eigenvalue E_i cannot be made smaller within the desired accuracy. To minimize the number of calculations needed, it is convenient to choose the next β near the minimum of a second-order polynomial curve constructed from a fit of the "best" three (β,E_i) points.

(v) The basis set is enlarged, a new value for the parameter β is chosen, and steps (ii)–(v) are repeated until the selected eigenvalue cannot be made smaller within the desired accuracy.

Binding energies calculated in this manner for the first image-potential state at Cu (111), (100), and (110) surfaces are given in Fig. 2 for corrugation heights $2A$ of 0, 0.25, and 0.5 Å. The spacings of the surface corrugations were taken to be $(\sqrt{6}/4)a_{\text{lat}}$, $a_{\text{lat}}/\sqrt{2}$, and a_{lat} for the (111), (100), and (110) surfaces, respectively, where $a_{\text{lat}}=3.615$ Å is the lattice constant for Cu. The binding energies were found to be much reduced from their hydrogenic values for basis sets with $M=0$, but to recover nearly to the values shown here for basis sets with $M=1$. Accuracy to three significant figures was attained for the ground-state binding energies (in eV) by the use of basis sets having $M=4$ or 5 and $N=7$ or 8. Figure 2 shows that the binding energy decreases with increasing corrugation amplitude and with increasing frequency. It should be noted that in general the corrugation amplitude is smaller (greater) for crystal surfaces with greater (smaller) corrugation frequency.

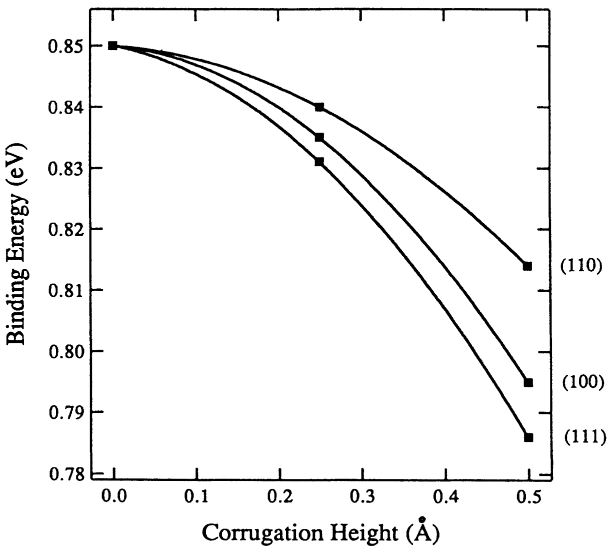

FIG. 2. Calculated binding energy of the ground image-potential state as a function of surface corrugation height for Cu(110), Cu(100), and Cu(111) crystallographic surfaces. The energies determined for corrugation heights of 0, 0.25, and 0.5 Å are connected by smooth curves to guide the eye.

Clearly, in this simple model the hydrogenic binding energies are little affected by surface corrugations. This contribution is in fact much less than the energy differences between materials for a given surface crystallographic structure, and is comparable to the uncertainty in the experimentally determined work functions used to find the vacuum energy levels from which the image-state binding energies are measured. Just as happens at a real crystal surface, the electron wave functions conform to the surface structure in such a way as to minimize their energy, thereby minimizing the effects of that structure. It seems unlikely that use of a more realistic potential—one that joins smoothly to the crystal bulk potential and allows the image-state wave functions to decay inside the surface—will alter these results appreciably.

ACKNOWLEDGMENTS

This work was supported in part by the U.S. Department of Energy through the Exploratory Research and Development Program at EG&G Idaho, Inc.

---

[1] K. Giesen, F. Hage, F. J. Himpsel, H. J. Riess, and W. Steinmann, Phys. Rev. Lett. **55**, 300 (1985).

[2] K. Giesen, F. Hage, F. J. Himpsel, H. J. Riess, and W. Steinmann, Phys. Rev. B **33**, 5241 (1986).

[3] K. Giesen, F. Hage, F. J. Himpsel, H. J. Riess, and W. Steinmann, Phys. Rev. B **35**, 971 (1987).

[4] K. Giesen, F. Hage, F. J. Himpsel, H. J. Riess, W. Steinmann, and N. V. Smith, Phys. Rev. B **35**, 975 (1987).

[5] D. Straub and F. J. Himpsel, Phys. Rev. B **33**, 2256 (1986).

[6] M. Ortuño and P. M. Echenique, Phys. Rev. B **34**, 5199 (1986).

[7] N. V. Smith, Appl. Surf. Sci. **22/23**, 349 (1985).

[8] N. V. Smith, Phys. Rev. B **32**, 3549 (1985).

[9] P. M. Echenique and J. B. Pendry, J. Phys. C **11**, 2065 (1978).

[10] E. G. McRae, Rev. Mod. Phys. **51**, 541 (1979).

[11] N. Garcia, B. Reihl, K. H. Frank, and A. R. Williams, Phys. Rev. Lett. **54**, 591 (1985).

[12] G. Binnig, K. H. Frank, H. Fuchs, N. Garcia, B. Reihl, H. Rohrer, F. Salvan, and A. R. Williams, Phys. Rev. Lett. **55**, 991 (1985).

[13] W. L. Clinton, M. A. Esrick, and W. S. Sacks, Phys. Rev. B **35**, 4074 (1987).

[14] S. L. Hulbert, P. D. Johnson, M. Weinert, and R. F. Garrett, Phys. Rev. B **33**, 760 (1986).

[15] D. B. MacMillen and U. Landman, J. Chem. Phys. **80**, 1691 (1984).

[16] S. T. Epstein, *The Variational Method in Quantum Chemistry* (Academic, New York, 1974).

[17] V. B. Shikin, Sov. Phys.—JETP **33**, 387 (1971) [Zh. Eksp. Teor. Fiz. **60**, 713 (1971)].

[18] R. M. Nieminen and M. J. Puska, Phys. Rev. Lett. **50**, 281 (1983).

[19] R. Loudon, Am. J. Phys. **27**, 649 (1959).

[20] D. ter Haar, *Selected Problems in Quantum Mechanics* (Academic, New York, 1964), p. 106.